Experimental Evaluation of a High Test Peroxide Catalyst Chamber for a Hybrid Rocket Engine

Ognjan Božić, Daniel Lancelle*, Stefan May* and Dennis Porrmann**
**DLR, German Aerospace Center, Institute of Aerodynamics and Flow Technology, Braunschweig, Germany*

Abstract
Hybrid rocket propulsion technology has recently gained in importance. Within the program "AHRES" at the German Aerospace Center (DLR), a small HRE technology demonstrator was developed, which should deliver data for the validation of a self-developed HRE design software. Instead of a conventional ignition system, for this HRE a catalyst chamber with a silver mesh catalyst is designed to decompose currently up to 0.7 kg/s of 87.5% HTP to steam and oxygen at high temperatures.

The chamber consists of the catalyst itself, a mount for the catalyst material, a retainer, an injector manifold, a cooling channel, and a casing. Furthermore, a pressure sensor, a mass flow sensor, and a thermocouple are attached to measure the properties of the decomposition products. The chamber is mounted on a test-bed which comprises attachment, peroxide storage, feed system, valves, data acquisition, and control. By determination of the decomposition temperature, the integrity of decomposition is verified and compared to theoretical prediction. The catalyst chamber is developed based on the results of the design tool SHAKIRA. Several calculations are carried out to determine the appropriate geometry for complete decomposition with a minimum of catalyst material. The experimental results show good agreement to the results generated by the design tool.

The developed and tested catalyst chamber provides a simple, reliable ignition system for hybrid rocket engine based on hydrogen peroxide as oxidiser. The system is capable of igniting repeatedly without the need to meet an optimal ignition point. Such a system behaves like a hypergolic engine in terms of ignition, but no hazardous substances are required.

ABREVIATIONS

AHRES	- Advance Hybrid Rocket Engine Simulation
H_2O	- Water
H_2O_2	- Hydrogen peroxide
O_2	- Oxygen
HRE	- Hybrid Rocket Engine
HTPB	- Hydroxyl-Terminated Polybutadiene
HTP	- High Test Peroxide
LRE	- liquid rocket engine
NTO	- Dinitrogen Tetraoxide (N_2O_4)
RGTP	- Rocket Grade Test Peroxide
SHAKIRA	- **S**imulation of **H**igh test peroxide **A**dvanced (**K**)Catalytic **I**gnition system for **R**ocket **A**pplications

SYMBOLS (Latin)

A_0	$mol/(s \cdot kg_{cat} \cdot K^{1/2})$	zero order reaction constant
A_1	$m^3/(s \cdot kg_{cat} \cdot K^{1/2})$	first order reaction constant
c_p	J/(kg K)	specific heat capacity by constant pressure
c_v	J/(kg K)	specific heat capacity by constant volume
c*	m/s	characteristic velocity
$E_{a,cat}$	J/mol	Arrhenius activation energy of HTP reaction

$\dot{m}$	kg/s	mass flow
$\dot{r}$	kg/s	decomposition rate
$M_{H_2O_2}$	kg/mol	HTP molar mass
p_c	bar	pressure in the catalytic chamber
R	J/(K mol)	universal gas constant
R_i	J/(kg K)	specific gas constant
T	K	local temperature in catalyst bed
T_{ad}	K	adiabatic temperature
T_{env}	K	environment/ ambient temperature
T_{exp}	K	experimental temperature (measured)
T_{ad}	K	adiabatic temperature

SYMBOLS (Greek)

$\rho_{H_2O_2}$	kg/m^3	HTP density
Γ	–	Vandenkerckhove function
$\eta_{\Delta T}$	–	Temperature efficiency
η_{c^*}	–	Characteristic velocity efficiency
κ	-	Ratio c_p/c_v
ΔT	K	temperature difference
ω_{H2O2}	-	local mass fraction of H_2O_2

Important indices

ad	adiabatic
CB	catalyst bed
exp	experimental
env	environment
FL	feed line
max	maximum
mean	medium
ox	oxidizer
theo	theoretic

1. Introduction

Hydrogen peroxide as oxidizer for rocket bi-propellant or mono-propellant engines has been in use for 70 years. The long history of HTP application includes the German V-2 projectile in Second World War, the British "Black Knight" in the 1960's, the USA rocket plane X-15 (for turbine drive), and the Russian Soyuz launcher (also as turbine drive of LOx/kerosene booster). Furthermore, in the 1950's, Rocketdyne Company developed the liquid rocket engine AR2 (90% HTP), and successfully applied it to enhance jet fighter aircraft for many years. Over years the use of HTP (RGTP) on aerospace was suppressed due to the utilisation of hydrazine (for monopropellant applications) and dinitrogen tetraoxide (NTO), which has a slightly higher specific impulse. However, these rocket propellants are poisonous, carcinogenic, and bring out health and safety risks during production, storage, transport, and handling. In the last decade HTP, as a green propellant, again became an attractive option and promises to substitute hydrazine and NTO, especially for rocket engines with small and medium thrust loads.

In the last 15 years a number of companies, research institutions, and universities worldwide have investigated catalytic / combustion properties of HTP and applied it to different rocket propulsion systems [e.g. Rocketdyne (USA), NASA – J. Stennis (USA), Purdue University – W. Lafayette (IN, USA), General Kinetics (CA, USA), Herakles - Safran (F), ONERA (F), DLR – AS Braunschweig (D); ALTA S.p.A., Pisa (I), University Road - Southampton (UK), Defence Agency for Technology - Seoul, (S. Korea), and a number of universities and research institutions in China]. Rocket engines based on HTP as oxidizer can be used for satellites propulsion (in mono- or liquid bi-propellant systems), as a thruster for LRE launcher booster and HRE/LRE upper stages, moon landers, sounding rockets, rocket airplanes for space tourism, or for investigation of the upper Earth atmosphere layers. One additional HTP application recently investigated by several institutions in last time is a catalytic HTP ignition system

for LRE and HRE, which represents a cheap and reliable solution. The use of HTP for hybrid rocket engines [16] has several positive consequences:

- a separate ignition system is not necessary,
- structure/propellant mass ratio is lower than for other propellant mixtures,
- regression rate of solid fuel grain is higher compared to large number of known propellant mixtures, which enables corresponding higher thrust,
- the throttling of the engine can be efficiently realised by mass flow control of the HTP oxidizer,
- the specific impulse for 92% HTP based propellant mixtures are equal or superior to corresponding mixtures with NTO and only 8% lower than for corresponding mixtures with oxygen.
- by holding a valid technical and security regulations for work with HTP, the risk of fire, explosion, or personal injuries is lower than for other high energy propellant combinations.

These arguments delivered the basics for the start of the DLR program "AHRES". This program also includes development and tests with a hybrid rocket engine demonstrator, based on hydroxyl-terminated polybutadiene with metallic additives as solid fuel and high concentrated hydrogen peroxide (HTP) as liquid oxidiser [16]. Instead of a conventional ignition system, a catalyst chamber with a silver mesh catalyst is designed to decompose the HTP to steam and oxygen at very high temperature. The catalyst chamber is able to decompose currently up to 0.7 kg/s of 87.5% HTP and in the future more than 1 kg/s. Used as a monopropellant thruster, this results in a thrust of 1400 N at sea level. The first test results realised in pulsed mode with this catalyst chamber are presented in this paper.

2. Simulation model

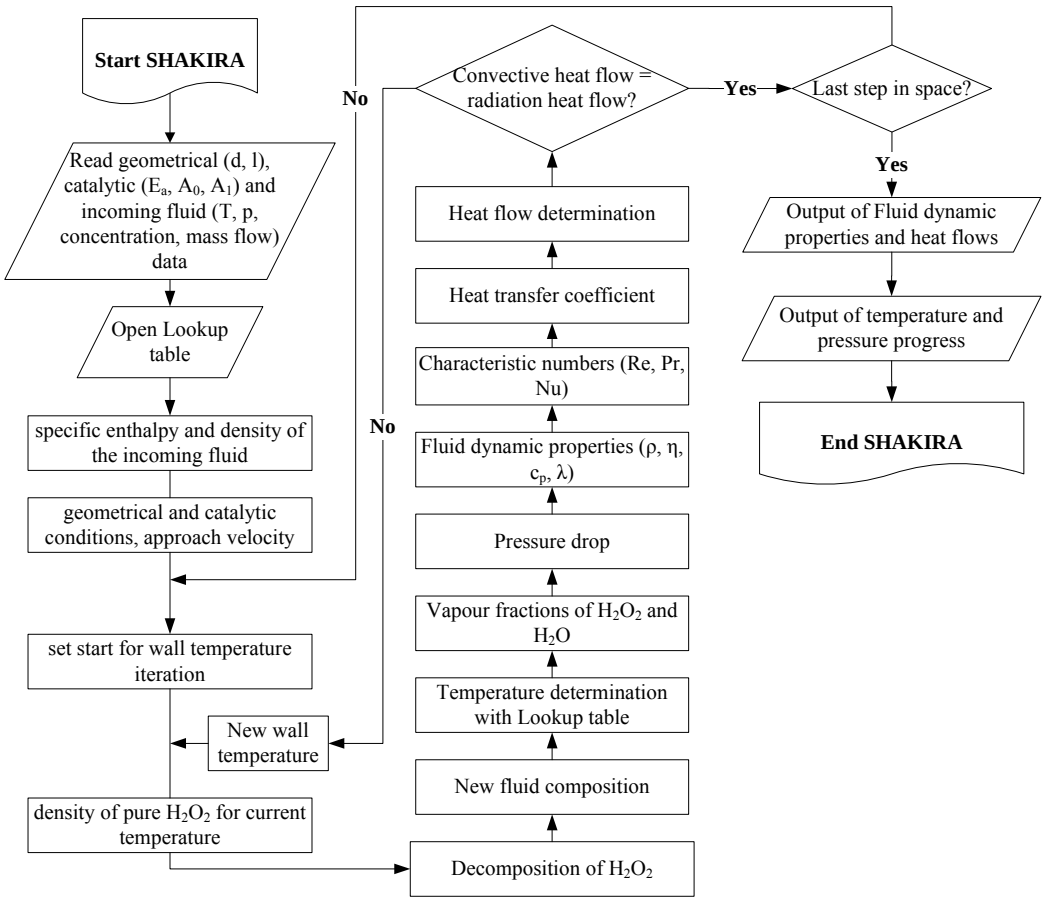

Figure 1: Flowchart of the program code SHAKIRA

To design a catalyst chamber for decomposing HTP, the 1-D simulation code SHAKIRA (**S**imulation of **H**igh test peroxide **A**dvanced (**K**)Catalytic **I**gnition system for **R**ocket **A**pplications) is developed. The catalyst chamber is

idealized as a symmetric hollow cylinder with ideally homogenous medium conditions in the volume of each grid element. These spatial steps are defined by discretisation of the chamber in axial direction. In the first step, initial conditions (media temperature T, pressure p, weight concentration of hydrogen peroxide ω_{H2O2}, mass flow $\dot{m}$) are required. After that, calculations are carried out based on results of the last step. The essential expression in the model SHAKIRA is the equation to determine the decomposition rate $\dot{r}$:

$$\dot{r} = m_{cat} \cdot M_{H_2O_2} \cdot \left(A_0 + A_1 \cdot \omega_{H_2O_2} \cdot \frac{\rho_{H_2O_2}(T)}{M_{H_2O_2}} \right) \cdot \sqrt{T} \cdot exp\left(-\frac{E_{a,cat}}{R \cdot T} \right) \quad (1)$$

with the molar mass M_{H2O2}, the effective catalyst mass m_{cat}, the zero order reaction factor A_0, the first order reaction factor A_1, the universal gas constant R, the density ρ_{H2O2} and the catalytic material depending reaction activation energy $E_{a,cat}$. The effective catalyst mass depends on the material and the geometry of the catalyst. This model can be used to determine many different catalytic materials and two different geometries (meshes and pebble beds) of the catalyst material itself. Detailed description of the program code is given in the literature [14]. The flowchart of SHAKIRA is shown in Figure 1.

In the predesign phase of the AHRES program, different options for the catalyst bed are determined (e.g. platinum coated spheres, monolithic platinum based catalyst, perovskite based materials such as $La_{0,8}Sr_{0,2}CoO_3$ - referred as LSC). Due to the high costs of alternative catalyst materials and manufacturing complexity, in the first development step the catalytic chamber is equipped with silver meshes. They are easy to obtain, relatively cheap, and have excellent advantages as a catalyst. In respect of its melting point, silver is applicable up to a concentration of 92 wt. % of H_2O_2. Therefore, calculations with SHAKIRA for a chamber with a catalyst of mesh geometry and silver as catalytic material are carried out with a mass flow of 0.7 kg/s, a HTP concentration of 87.5 wt. % and an inner chamber diameter of 0.1 m. The simulation results are shown in Figure 2. The evolution of the effective decomposition rate of H_2O_2 for each step and the evolution of media temperature are plotted in Figure 2a. Additionally, the mass fractions of the three species H_2O_2, H_2O and O_2 and the vapor fractions for H_2O_2 and H_2O, which are related to maximum vapor content at process completion of every single species, are shown in Figure 2b.

At first, the temperature and decomposition curves show a very flat progression and the decomposition rate is very low. After about 30 mm, the decomposition rate increases as a result of the significantly growing temperature. Past a short peak close to 42 mm, the decomposition rate decreases and the temperature stays at a plateau of almost 403 K. The reason for this behavior is that at nearly 42 mm the liquid mixture is starting to boil (see Figure 2b) and in that case, the average density of the medium, and also the density of pure H_2O_2, significantly decreases. This means the number of H_2O_2 molecules per volume is reduced. In accordance with Equation 1, the decomposition rate diminishes drastically. After about 56 mm, the whole medium is vaporized and the temperature increases again. Due to the exponential correlation between decomposition rate and medium temperature, the decomposition rate grows strongly. Thus, at nearly 65 mm, the H_2O_2 is completely decomposed into hot steam and oxygen.

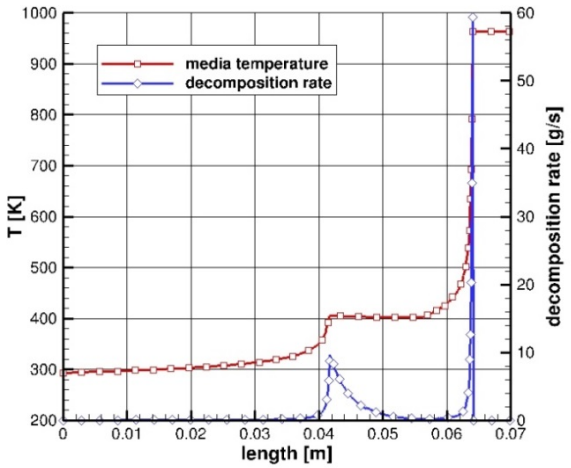

Fig. 2a: Decomposition rate and medium temperature vs length for a catalyst chamber with silver meshes

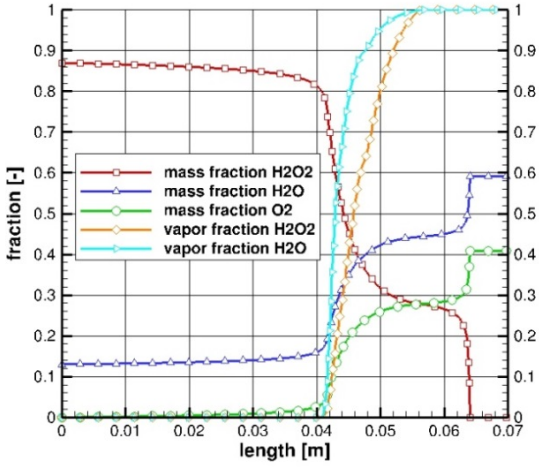

Fig. 2b: Mass and vapor fractions for the three species H_2O_2, H_2O and O_2 vs length for a catalyst chamber with silver meshes

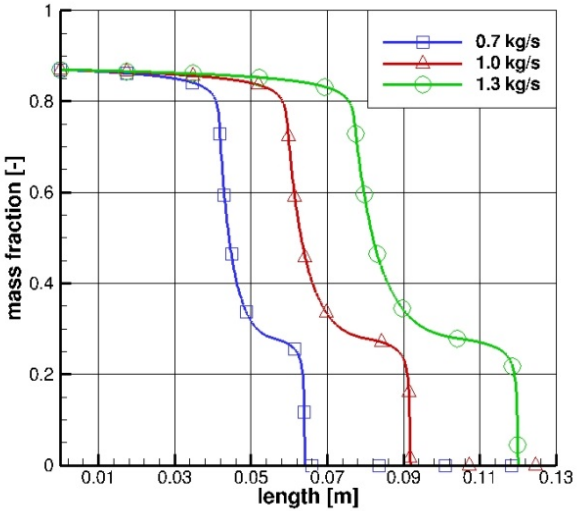

Figure 3: Mass fractions of H_2O_2 vs length for different mass flows

The effective length of the designed catalyst chamber is up to 0.13 m. In Figure 3, the mass fraction of H_2O_2 vs. the distance from the inlet for a mass flow of 0.7 kg/s, 1.0 kg/s and 1.3 kg/s are plotted. This shows clearly that a higher HTP mass flow up to 1.3 kg/s could be completely decomposed within the designed catalyst chamber. In forthcoming project steps, this capacity will be tested and used.

3. Constructed catalyst chamber

Within the AHRES program the developed catalytic chamber is a modular robust solution which enables tests with different catalyst bed solutions for high HTP chamber pressures up to 70 bars. The presented design is primarily intended as preheated steam/gas generator with the aim to supply the discussed hybrid rocket engine demonstrator with gasified oxidizer and to enable multiple ignition of the engine without a separate ignition system.

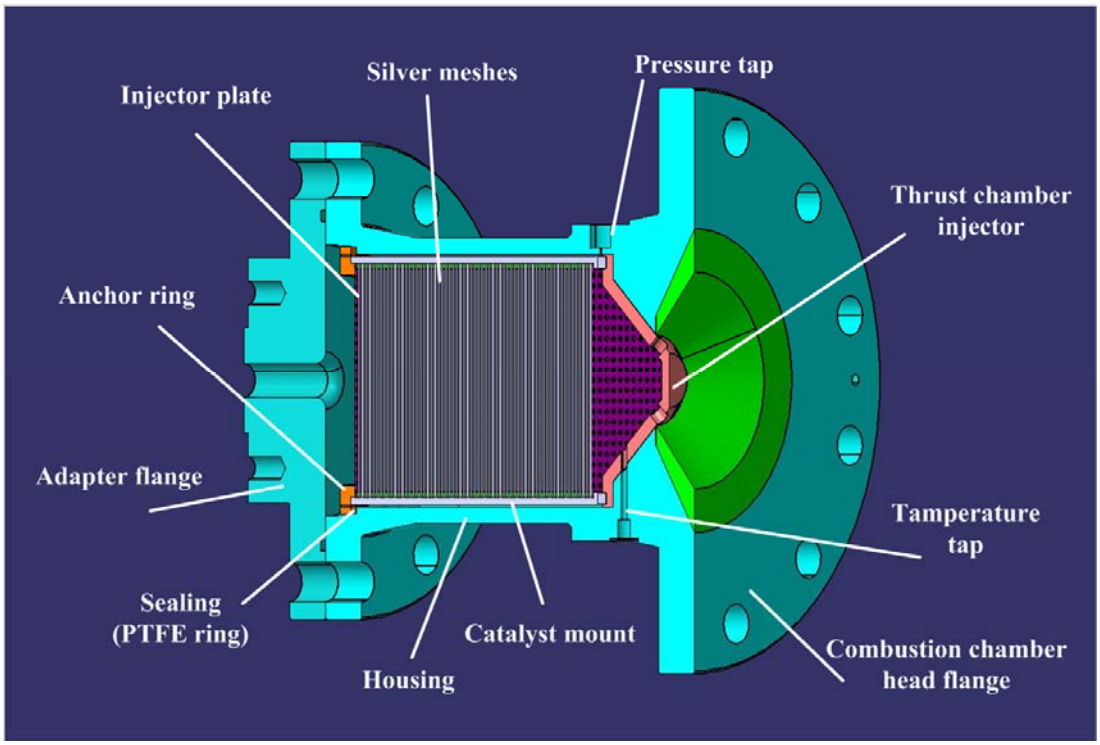

Figure 4: Catalytic chamber for AHRES hybrid rocket engine

The established and proved catalyst chamber solution could also be upgraded to a HTP monopropellant thruster for different purposes, with moderate effort [10], [11], [13].

The catalyst chamber housing is made out of alloy Inconel 718 to meet all future investigation requirements, and it is rated for HTP concentrations up to 98 %wt. At the left and right ends of the housing, connectors are incorporated (s. Fig. 4) to enable a good sealing and more security for repeated connection/ disconnection of design elements as is common during research activities. On the left connection side (in direction of the HTP feeding line) a flat sealing gasket, made out of Teflon based plastic, is mounted. To reduce the number of connection elements, which again reduces the security risks through bad sealing under dynamic operational conditions, the catalyst chamber is designed as monoblock construction with an injector head for the HRE combustion chamber.

The catalyst mount, formed as cylindrical tube with an inner diameter of 100 mm, is inserted into the casing. The mount fulfils two main functional roles. It serves as mechanical protection for the catalyst bed. The catalyst bed consists of high purity silver screens. The silver mesh has 32x32 knitting holes per square inches of silver wire with a diameter of 0.27 mm. Depending on the required HTP mass flow, up to 250 silver screens can be embedded within the catalyst mount. In current tests up to 142 catalyst silver screens were used. To prevent mesh deformation or break-up due to pressure pulses on the upper side (flow feeding side), a distribution plate is attached. On the bottom side, a support plate with a large number of holes is installed. Between the catalyst mounting and the catalyst chamber housing there exists a cylindrical gap. During the tests this gap contributes to the reduction of heat transfer between flowing liquid HTP/decomposition products within mounting and the housing. This reduces the ramp-up time until steady state working conditions are reached. The implemented design enables flexible handling with catalyst beds composed of heterogeneous structures or different catalyst materials. This is especially attractive for HTP applications with concentrations higher than 87.5%wt.

4. Description of the feed system

The main part of pressure feeding system of HTP-oxidizer is the high-pressure tank (s. Fig. 5). It is mounted on a stainless steel plate equipped with four force sensors, which enables the measurement of instantaneous HTP filling weight. As a redundant system, the filling level can be determined by an ultrasonic probe mounted at the base of the pressure vessel. The HTP tank is equipped with six flange connectors: four on the lateral side and one each on the top cover plate and the bottom tank side.

On one of the lateral connection a solenoid valve (V9) is attached, which in the open state allows the charging of the tank by means of a volumetric dosing pump. On the second lateral connection, a multi-branched manifold (pipe crossing) is mounted to connect one further solenoid valve for pressure discharge (V5), one mechanical ball valve for manual emergency pressure blow off (V12), as well as one solenoid valve for tank pressurization with nitrogen up to 100 bar (V3). The necessary nitrogen flow of 0.33 m_n^3/s for the tank supply is assured using a battery of nitrogen bottles with 200 bar and 300 bar, equipped with a robust systems of control valves.

On the third lateral tank connection one further solenoid valve (V7) is attached, which enables flush/purge of tank and feed system with high purity water before and after the tests. The permanent supply of filtered high purity water (on demand) is assured by one ion exchanger attached on the fourth lateral tank connector. The ion exchanger is connected to the water supply grid. The manually controlled ball valve (V13) allows extraction of high purity water for cleaning of the transport canister and the catalyst chamber and hybrid engine parts after the tests. On the fourth flange connector, a T-fitting is fixed for housing two thermocouples and one pressure sensor for the supervision of the HTP pressure vessel. An excess pressure valve is attached on the tank cover plate, which opens at pressures higher than 120 bars to prevent tank burst. Safety tests show that the tank can withstand pressure loads up to 180 bars without stress or deformation overloads. The tank base includes the operation port for HTP extraction. On the port flange a T-fitting is mounted, which enables attachment of a manually controlled discharge valve (V11) and a solenoid valve (V1) which in open state permits HTP feeding in direction of the catalyst chamber. In emergency cases, the discharge valve (V11) enables the HTP to be directed over one specially designed high pressure discharge nozzle (D1) in the dump basin.

At the main pipe line for HTP feeding between the valve (V1) and the catalyst chamber several control elements and measurement sensors/ instruments are attached. Behind the valve (V1) in the pipe line a pneumatically driven control valve (V10), a Coriolis flow meter, a check valve (V15), and a 3/2-way valve (V2) are installed. The combination of the control valve (V10) and the Coriolis sensor enable a precision HTP flow setting.

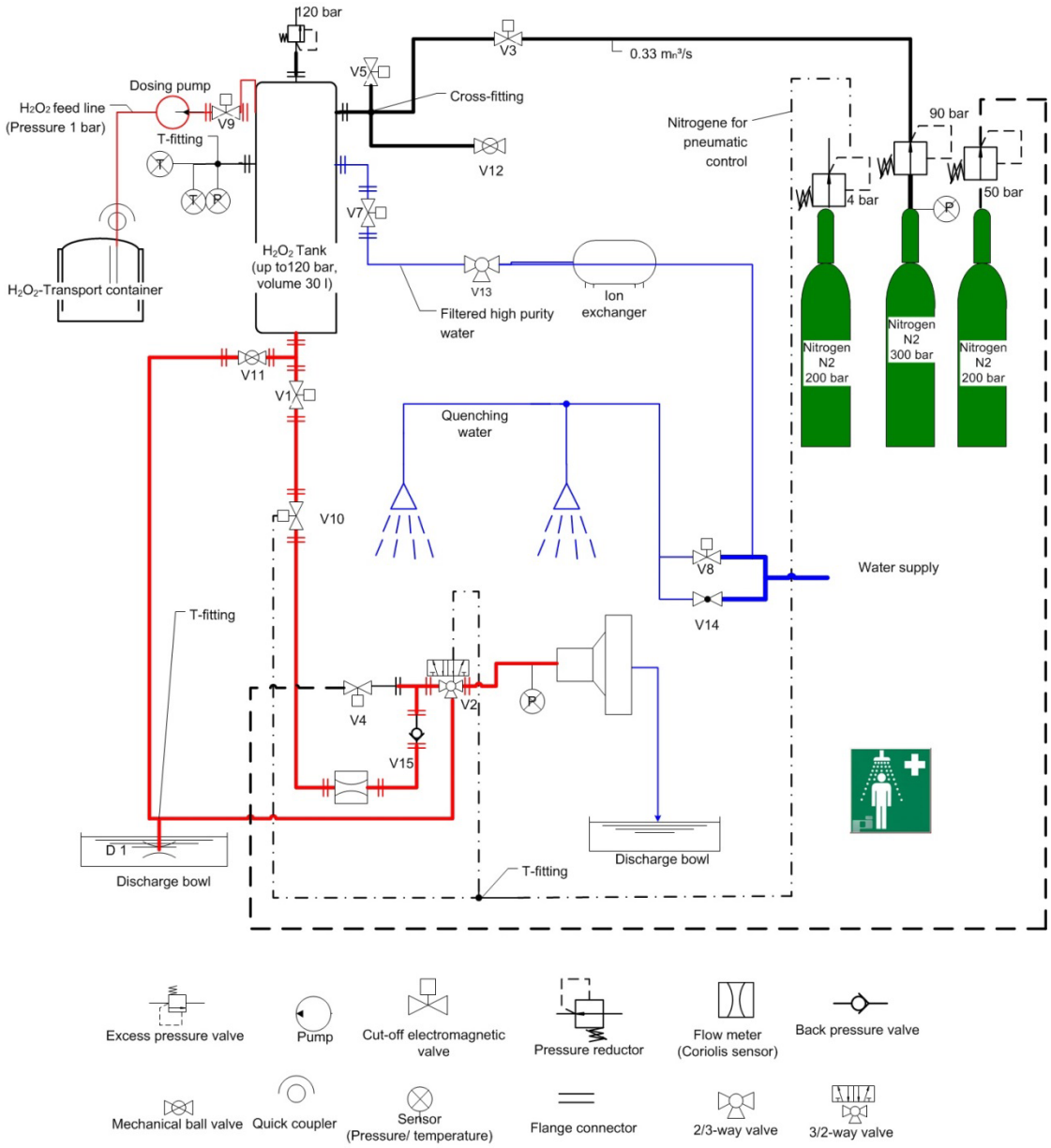

Figure 5: H_2O_2 – Flowchart (HRE Test bed)

The check valve (V15) prevents pressure shock spreading from the catalyst/engine chamber in the direction of the feed line and tank. Between the valves (V15) and (V2) a T-fitting is attached. On its third free connection a solenoid valve (V4) is installed. In the open state the valve (V4) enables feeding nitrogen with a pressure of 50 bar into the catalyst or engine chamber, and thus drying or clean-up of catalytic chamber or extinction of the HRE combustion chamber (if attached).

After completion of the test the valve (V2) guides the flow in the direction of the dump basin. This enables the system to be cleaned of accumulated waste HTP. The spraying of HTP in the dump basin is prevented by a discharge nozzle (D1). All solenoid valves, which are in direct contact to the HTP, are of the coaxial type.

5. Applied measurement technique

Two pressure sensors are connected in the oxidizer feed line, one in front of the catalytic chamber and one at the catalytic chamber housing – in front of catalyst injector (s. Fig. 6). The difference of these two pressure values equals the pressure loss across the catalyst chamber.

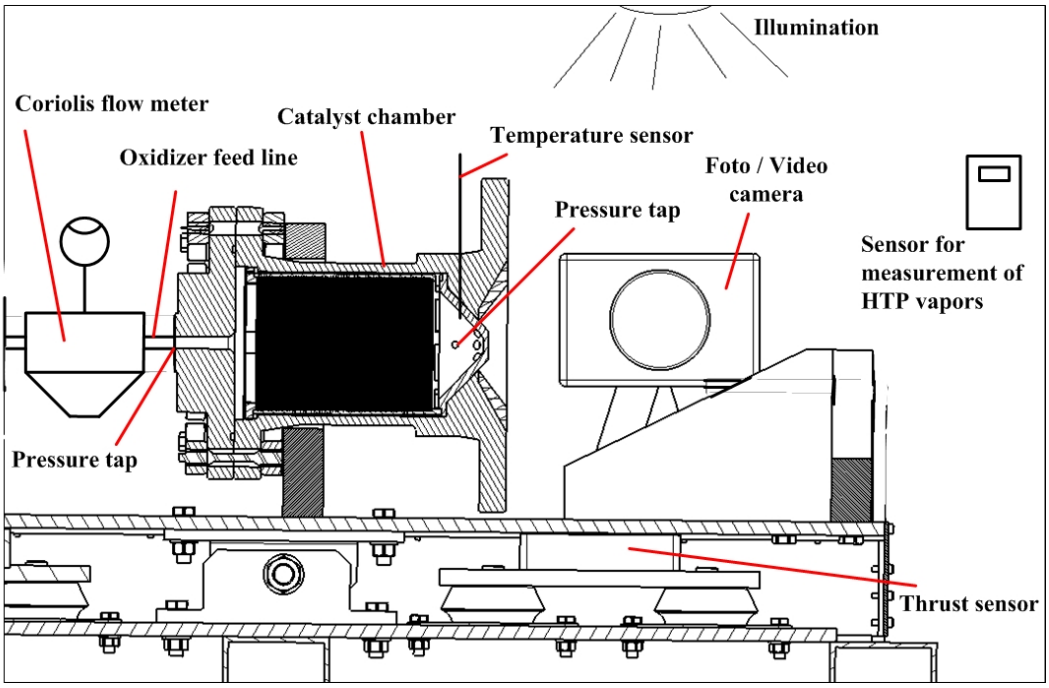

Figure 6: Arrangement for testing of HTP catalytic chamber

Both pressure sensors (KTE6000), delivered from "Sensortechnics", are of the membrane type and have a measurement range of 0-150 bar and 0-100 bar respectively. On the back side of the catalyst bed and in front of chamber injector a shielded thermocouple of type N with a measurement range of 1200°C is attached. Despite of the fact that the catalytic chamber has no classic convergent-divergent nozzle, but rather a sonic injector on the exit, it was possible to measure the thrust force on the test bed. With a system of four photo and video cameras, the form and length of the exhaust steam/oxygen jet is optically registered. The concentration of hydrogen peroxide vapour is measured with a HTP gas detector of type Dräger Pac III with the sensor XS EC H_2O_2 for a measurement range of 0-20ppm. Concentration of liquid HTP is controlled indirectly by density measurement. The temperature of liquid HTP before inflow in the catalyst chamber is also measured with type J thermocouple. The HTP mass flow measurement is realized with a Coriolis flow meter obtained from Kobold Messring GmbH TMU – 010 (measurement range 0 – 0.7 kg/s).

Figure 7: DLR test facility for hybrid rocket engines at Trauen - Fassberg, Germany

6. Preliminary test results

The presented preliminary results are attained during a measurement campaign carried out at the DLR test range Trauen - Fassberg in March 2013 (s. Fig. 7). Three of four experiments were successfully completed and post-analysis and evaluation was done. During the fourth experiment the mass flow exceeded the measurement range of flow meter of 700 g/s, so it couldn't be evaluated. Despite this, tracking other measurement parameters showed that the process was completed with successes. Emission of HTP vapour outside the catalyst chamber during all experiments is not observed and it can be concluded that the decomposition process was finished.
Evaluation of the HTP catalyst chamber efficiency is carried out by means of the characteristic velocity efficiency η_{c^*} and the temperature efficiency $\eta_{\Delta T}$. The characteristic velocity efficiency η_{c^*} is an important criterion for estimating the energetic efficiency of the catalytic chamber. It can be given with the following expression:

$$\eta_{c^*} = \frac{c^*_{exp}}{c^*_{theo}} \tag{2}$$

The experimental value of characteristic velocity c^*_{exp} is determined with the expression

$$c^*_{exp} = \frac{\sqrt{R_i T_{exp}}}{\Gamma} \tag{3}$$

In equation (3) T_{exp} is the measured temperature of the decomposed gas mixture behind the catalyst bed in the catalyst chamber. In gas dynamic theory, the value Γ is known as the Vandenkerckhove function

$$\Gamma = \sqrt{\kappa \left(\frac{2}{\kappa+1}\right)^{\frac{k+1}{2(k-1)}}} \tag{4}$$

The catalyst bed is well isolated from the housing by means of a gap between the housing and the catalyst mount (s. Fig. 4). Because of this, the polytrophic constant $n = (c_p/c_v)_{diabatic}$ in the first approximation can be taken as equal to the adiabatic constant κ and can be used for calculation of expressions (3) and (4). The alternative calculation of c^*_{exp} using the equation

$$c^*_{exp} = p_c^{exp}.A_t/\dot{m}_{exp} \tag{5}$$

is not suitable, because the applied catalyst chamber has no convergent-divergent nozzle on the exit, as is usual for monopropellant HTP rocket engines. The flow conditions in vicinity of the 8 injectors (with sharp edges at the entrance side) don't correspond well with throat conditions in the nozzle.

The theoretical values of decomposition temperature T_{ad} and c^*_{theo} are determined with Gordon – McBride CEA2 Thermochemistry code [17]. In the code the relationship between named variables are also based on the formulation

$$c^*_{theo} = \frac{\sqrt{R_i T_{ad}}}{\Gamma} \tag{6}$$

For the HTP PROPULSE 875 (Evonik, Deutschland) with H_2O_2 concentration of 87.5 %wt, the adiabatic decomposition temperature is T_{ad} = 968.46 K and the theoretical characteristic velocity is c^*_{theo}=913 m/s. With CEA code, the calculated values for T_{ad} and c^*_{theo} don't show any change with pressure increase, but in reality discrepancies of few percent, dependent of pressure level in the chamber, are possible [18]. The measured temperature T_{exp} , as well as the corresponding value c^*_{exp} are lower (s. Table 1) than the calculated theoretical values. This can be explained by the losses due to the cooling in the injector/ chamber head area downstream the catalyst bed and the discrepancy between ideal 1D-expansion/real expansion of decomposed gas products in the convergent injector cone.

One additional indicator for estimating the efficiency of the catalytic chamber is the temperature efficiency

$$\eta_{\Delta T} = \frac{T_{exp} - T_{env}}{T_{ad} - T_{env}} \tag{7}$$

The two further important operational criteria for characterisations of a catalytic chamber are the pressure drop across the catalyst bed Δp_{CB} and the total pressure drop across the feed line Δp_{FL} (between oxidizer tank and injector

on HRE combustor head). They have important influence on decomposition process stability and structure weight (catalyst chamber and whole oxidizer feeding system).

Table 1: Estimated efficiency of catalyst chamber during carried tests

			Test 1	Test 2	Test 3
Mass flow - measured	$\dot{m}_{exp}$	(kg/s)	0,272	0,412	0,532
Process time	τ	(s)	6	8	9
Characteristic velocity [experim. value]	c^*_{exp}	(m/s)	823,90	842,56	840,45
Chamber pressure	p_c	(bar)	8,16	13,5	17,36
Mean temperature efficiency	$\eta_{\Delta T,\ mean}$	(%)	73,59	78,80	78,22
Maximum temperature efficiency	$\eta_{\Delta T,max}$	(%)	84,75	86,77	88,56
Mean characteristic velocity efficiency	$\eta_{c^*,\ mean}$	(%)	90,10	92,14	91,91
Maximum characteristic velocity efficiency	$\eta_{c^*,\ max}$	(%)	94,41	95,17	95,82
Total pressure drop across feed line	Δp_{FL}	(bar)	20,44	14,6	22,64
Pressure drop through the catalyst bed	Δp_{CB}	(bar)	0,5	0,71	1,01

The results of the measured efficiency criterions are given in table 1. The mean temperature efficiency $\eta_{\Delta T,\ mean}$ is in the range of 73,6 to 78,2%. Maximum temperature efficiency $\eta_{\Delta T,\ mean}$ is in the range of 84,8 to 88,6%. During all tests, the mean characteristic velocity efficiency $\eta_{c^*,\ mean}$ exceeds 90% and maximum characteristic velocity efficiency $\eta_{c^*,\ max}$ (%) is in the vicinity of 95%. All these parameters are realized by a mass flow load of the catalyst chamber not more than 40% of the designed capacity. The conducted tests and analysis indicate that for high loads of the catalyst chamber with a HTP mass flow over 1 kg/s the efficiency criteria can be improved.

The reported tests with the catalyst chamber are carried out in the pulsed regime and for this reason were not fully steady. By application of relatively high HTP mass flows, the transition from start point to steady state need a period of up to 4 s. The same transition time is necessary to shut off the process from the moment when the control valve is closed. This is a consequence of accumulated HTP mass within the catalyst bed which must be exhausted. The maximum mass flow achieved in the presented test results (s. Fig. 8 to 10) is an indicator for possible steady state flow. This conclusion should be confirmed by forthcoming steady state tests with test durations up to 40 s. The mean values of efficiency criteria achieved in these experiments are more representative for the catalyst chamber under transient working conditions.

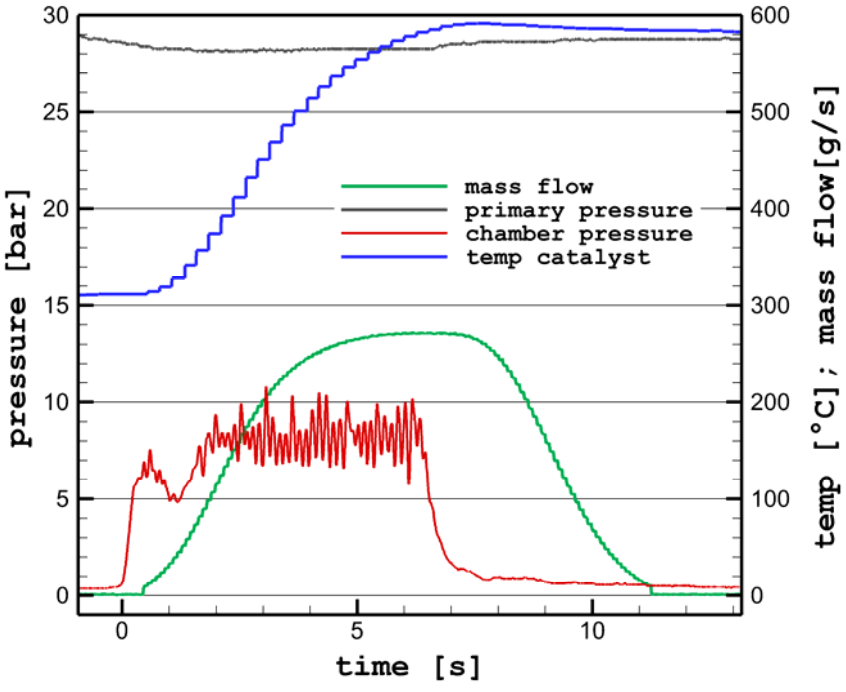

Figure 8: H_2O_2 catalytic chamber test (1) with main mass flow 272 g/s

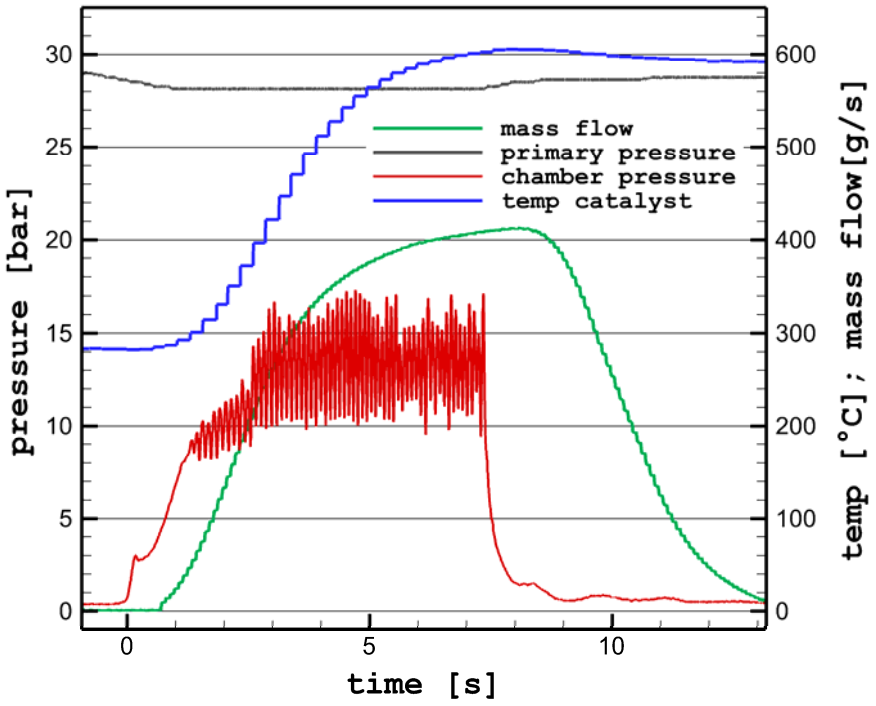

Figure 9: H_2O_2 catalytic chamber test (1) with main mass flow 412 g/s

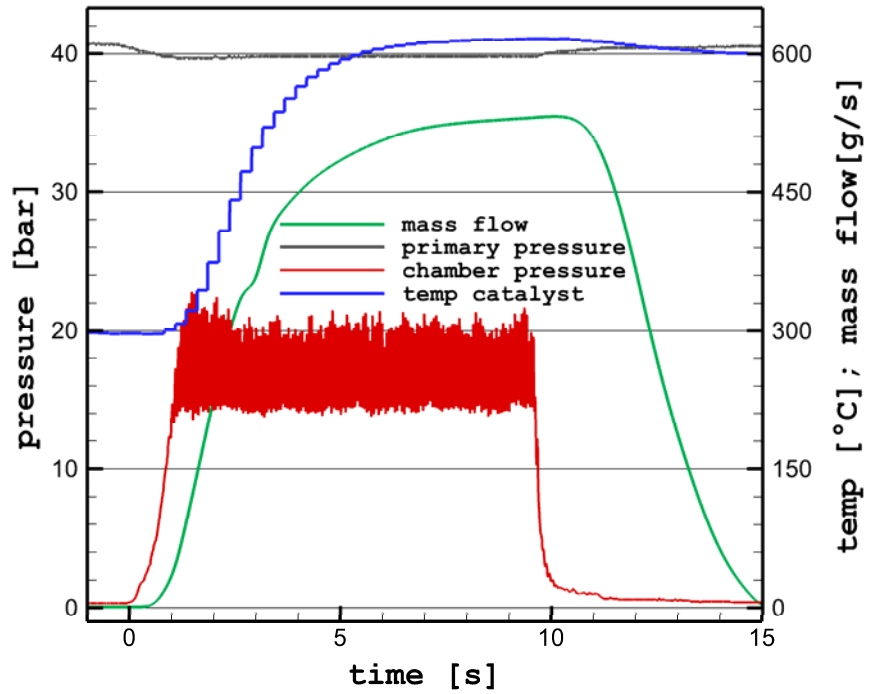

Figure 10: H_2O_2 catalytic chamber test (1) with main mass flow 532 g/s

The properties of the exhaust jets (s. Figures 11 and 12) are dependent on the mass flow value. At lower mass flows (generally under 120 g/s) exhaust jets cool faster and unsaturated water steam will be generated. That makes the jet clearly visible and non-transparent. For higher mass flows, the exhaust jet comprises sufficient energy to deliver water steam in overheated condition and the jet remains transparent and rarely visible.

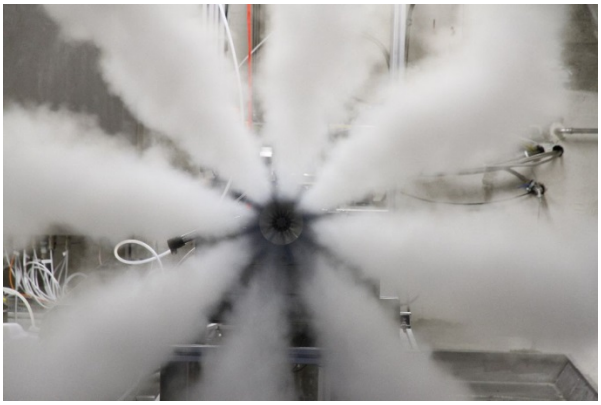

Figure 11: Test with HTP catalyst chamber carried out in December 2012 (mass flow 109,6 g/s)

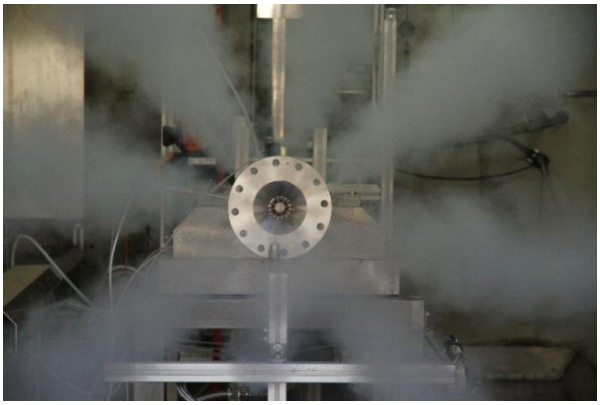

Figure 12: Test with HTP catalyst chamber carried out in March 2013 (mass flow 532 g/s)

Table 2: Properties of low frequency instabilities within catalyst chamber during tests

		Test 1	**Test 2**	**Test 3**
Mass flow	(kg/s)	0,272	0,412	0,532
Mean chamber pressure	(bar)	8,16	13,5	17,36
Frequency	(Hz)	6,3	8,86	18,0
Amplitude	(bar)	2,4	+5,5/-4,5	+6,64/-3,36

The diagrams on figures 8 to 10 and table 2 show the appearance of low-frequency instabilities with the frequencies between 6 and 18 Hz and amplitudes between 2,4 and 6,64 bar during the tests. The main reasons for the observed instabilities are the designed cavity length at the entrance of catalytic chamber and the design form of the injector plate with low pressure drop. The driving force due to coupling between feed system and vaporisation delay also has some influence during decomposition in the catalyst chamber. The degree of influence due this coupling cannot be estimated without further and more detailed tests. These instabilities are no problem for the robustly designed feed line and chamber itself, but could be a potential problem for the combustion chamber of the AHRES Hybrid rocket engine. Currently tests with another injector plate form and higher HTP mass flow are in preparation.

7. Conclusions

The tests carried out confirm the design functionality and flexibility of the catalyst chamber. Also, preliminary design requirements (e.g. HTP steady mass flow up to 550 g/s, complete decomposition of HTP in the water steam and oxygen without residue of hydrogen peroxide vapors, ignition temperature for HTPB exceeded) are achieved. An activated silver mesh catalyst pack works well with HTP PROPULSE 875. The decomposition temperature was 300°C below the melting point of silver. Furthermore, silver is cheap compared to platinum and has a good commercial availability.

In this paper the preliminary results of a test campaign carried out in spring 2013 are presented, with the goal to estimate the properties and the thermal efficiency of the catalyst chamber of HRE developed within DLR AHRES research program. Currently underway are new tests with improved chamber properties, which should damp the amplitude of low-frequency instabilities and change its frequency. Possible amplifications of the instabilities within HRE combustion chamber will be damped and a contamination of the catalyst bed structure due the combustion products, forced backwards from combustion chamber, will be prevented. The achieved characteristic velocity efficiency is satisfying, but from our point of view it will rise under steady-state working conditions.

References

[1] Walter, H. 1964. Studie über die Anwendung von Hochkonzentrierten Wasserstoffperoxyd (H2O2) als Oxidator in der dritten-Stufe des ELDO-Trägersystems und auf weiteren Gebieten der Raumfahrt, *Auftrag Nr. RFT 19, HELLMUTH WALTER GmbH, Kiel - Wik*

[2] Clapp, M. B. and M.W. Hunter. 1993. A Single Stage to Orbit Rocket with Non-Cryogenic Propellants, AIAA 93-2285, *29th AIAA Joint Propulsion Conference*,

[3] Osmon, R. V. 1969. An Experimental Investigation of a Lithium Aluminum Hydride-Hydrogen Peroxide Hybrid Rocket, Aerospace Chemical Engineering, Vol. 62, No. 61, No. 61, 1966, pp. 92-102

[4] Pugibet, M., H. Moutet. 1970. On the Use of Hydrogen Peroxide as Oxidizer in Hybrid Systems, *La Recherche Aerospatiale*, No. 132, pp. 15-31. Translated From French by NASA as TTF-13034, May, 1970

[5] Musker, A. J., J. J. Rusek, C. Kappenstein, G. T. Roberts. 2006. Hydrogen Peroxide – from Bridesmaid to Bride, *3rd ESA International Conference on Green Propellants for Space Propulsion*, Poitiers, France, 17–20 September 2006

[6] Nimmerfroh, N., E. Walz, C. Brossemer. 2001. PropulseTM Hydrogen Peroxide: Manufacture, Quality, Safety, Transportation and Handling, Int. Conference on Green Propellant for Space Propulsion - in combination with the *4th International Hydrogen Peroxide Propulsion Conference*, 20-22 June 2001, ESTEC, Noordwijk, The Netherlands

[7] Ventura, M. C. 2005. Long Term Storability of Hydrogen Peroxide, *41st AIAA/ASME/SAE/ ASEE Joint Propulsion Conference & Exhibit,* Tucson, AZ, July 10-13, 2005, AIAA-2005-4551

[8] Wernimont, E. J., S. D. Heister. 2000. Combustion Experiments in Hydrogene Peroxide/ Polyethylene Hybrid Rocket with Catalytic Ignition, *J. of Propulsion and Power*, Vol. 16, No. 2, March-April 2000

[9] Ventura, M. C. 2005. Long Term Storability of Hydrogen Peroxide, *41st AIAA/ASME/SAE/ASEE Joint Propulsion Conference & Exhibit*, Tucson, AZ, July 10-13, 2005, AIAA-2005-4551

[10] Torre, L., A. Pasini, L. Romeo, L. d'Agostiono. 2008. Firing Performance of Advanced Hydrogen Peroxide Catalytic Beds in a Monopropellant Thruster Prototype, *44st AIAA/ASME/SAE/ ASEE Joint Propulsion Conference & Exhibit,* 21-23 July 2008, Hartford, CT, AIAA 2008-4932

[11] Jonker, W. A., A. E. H. J. Mayer, B. T. C. Zandbergen. 2006. Development of a Rocket Engine Igniter Using the Catalytic Decomposition of Hydrogen Peroxide, Green Propellants, *3rd ESA International Conference on Green Propellants for Space Propulsion*, SP-635, Poitiers, France, 17–20 September 2006

[12] Lee, S. L., C.-W. Lee. 2009. Performance characteristics of silver Catalyst bed for hydrogen peroxide, Aerospace Science and Technology 13 (2009), pp. 12-17

[13] Neumaier, W. W. Jr., M. Wells, A. Brinkley, T. Talty. 2012. Development of a 90% Hydrogen Peroxide Mono-Propellant Propulsion System for the Warm Gas Test Article, *48th AIAA/ASME/SAE/ ASEE Joint Propulsion Conference & Exhibit,* 30July – 1 August 2012, Atlanta, Georgia, AIAA 2012-3755

[14] May, S., D. Lancelle, D. Porrmann. 2013. Mathematical Modeling of a High Test Peroxide Catalyst Chamber for Hybrid Rocket Engines, ODAS 2013, *13th ONERA-DLR Aerospace Symposium*, 27-29 Mai, Paris

[15] Farbar, E., J. Louvers, T. Kaya. 2007. Investigation of Metalized and Non-metalized HTPB/ Hydrogen Peroxide Hybrid Rockets, *J. of Propulsion and Power*, Vol. 23, No. 2, March-April 2007

[16] Božić, O., D. Porrmann, D. Lancelle, A. Hartwig. 2012. Program AHRES and its Contribution to Assess Features and Current Limitations of Hybrid Rocket Propulsion*, 63th Congres of International Astronautical Federation*, October 2012, Naples, Italy, IAC-12-C4.2.8

[17] Gordon, S., B. J. McBride. 2004. NASA - GLENN Chemical Equilibrium Program CEA2, May 21, 2004, Refs: NASA RP-1311 (Part 1), 1994 and NASA RP-1311 (Part 2), 1996

[18] Walsh, R. F., A. M. Sutton. 2002. Pressure Effects on Hydrogen Peroxide Decomposition Temperature, 5th Int'l Hydrogen Peroxide Propulsion Conference, Lafayete, IN, USA 15-19 September 2002, AFRL-PR-ED-TP-2002-203